Study on parameters optimization of silver nanoparticles biosynthesized using aqueous extract of *Imperata cylindrica*

Noor Najmi Bonnia[a,*], Mohd Azri Ab Rani[b], Afiza Ahmad Fairuzi[a]

[a]School of Physics and Material Science, Faculty of Applied Sciences, Universiti Teknologi MARA, 40460 Shah Alam, Selangor, Malaysia, emails: noornajmi@salam.uitm.edu.my (N.N. Bonnia), cafizaahmadfairuzi@yahoo.com (A.A. Fairuzi)
[b]School of Chemistry and Environment, Faculty of Applied Sciences, Universiti Teknologi MARA, 40460 Shah Alam, Selangor, Malaysia, email: azri@salam.uitm.edu.my

ABSTRACT

Biosynthesis of nanoparticles has gained great attention in moving towards an economic and environmentally friendly process. However, there is a limited number of studies that describe the parameters for tuning the dimension and geometry of nanoparticles in the biosynthesis process. Therefore, in this study, silver nanoparticles were synthesized by varying the synthesis parameters in aqueous extract of *Imperata cylindrica*. The particles were characterized by visual observation; color changes, UV-visible spectroscopy, dynamic light scattering, field scanning electron microscopy, energy-dispersive X-ray spectroscopy, and X-ray diffraction. Changing the parameters such as plant extract concentration, silver salt concentration, the temperature of biosynthesis and pH of reaction mixture influence the size and dispersion of the nanoparticles. The optimum parameters for synthesizing silver nanoparticles are 10% of aqueous extract, 10 mM of silver nitrate, pH 5.7 with a reaction temperature of 60°C. The synthesized silver nanoparticles are in spherical with a diameter below 100 nm.

Keywords: Biosynthesis; Silver nanoparticles; *Imperata cylindrica*; Optimization; Monodisperse

1. Introduction

Most properties of metal nanoparticle such as optical [1], magnetic [2], catalytic [3,4], and optoelectronic [5] are closely related in size and shape [6]. Generally, metal nanoparticles are produced via two routes, which are the physical and chemical approaches. Although these conventional synthesis protocols allow fine-tuning of the particles' size and shapes, the process suffers several drawbacks. For instance, a physical approach typically involves the use of a tube furnace which occupies a large space, consumes an enormous amount of energy and time to operate. On the other hand, chemical reduction employs highly deleterious organic solvents and surfactants which must be separated and removed from the final products [7]. Thus, a 'greener' method of synthesizing silver nanoparticles has been explored by previous researchers to remedy this problem. In the past, silver nanoparticles have been successfully synthesized by using numerous plant extracts such as *Garcinia indica* [8], *Pandanus amaryllifolius* [9], *Azadirachta indica* [10], *Allium cepa* [11] and *Thymbra spicata* [12].

Despite the excellent progress that has been made in the green synthesis of metal nanoparticles, there is not much information on controlling the shape and size of nanoparticles. Some studies report the connection of physical parameters on the formation of a vivid range of silver nanoparticles [13] but the optimum condition for producing monodisperse nanoparticles was rarely discussed. As each plant contains

* Corresponding author.

unique biogenic materials in a different amount, the optimum parameters for synthesis can be perplexing. In the present study, *Imperata cylindrica* (*I. cylindrica*) (L.) Beauv. or cogon grass was used as a green reducing and capping agent in the synthesis of silver nanoparticles. This plant was chosen due to its significant content of tannins, alkaloids, and flavonoids [14,15] which are useful in the synthesis of metal nanoparticles. The use of aqueous *I. cylindrica* extract is very practical and economical as this plant can be found easily thriving in Southeast Asia, the Philippines, China, and Japan [16]. Subsequent to our previous study [17], the current research aims to optimize the synthesis parameters which include; concentration of metallic precursor (AgNO$_3$) and plant extract, reaction temperature, and pH of the medium to produce monodisperse silver nanoparticles.

2. Experimental section

2.1. Reagent

Silver nitrate (chemical structure; AgNO$_3$, molecular weight; 169.87 g mol^{-1}, and purity; 99.0%) was obtained from Sigma-Aldrich Co. (3050 Spruce Street, St. Louis MO 63103, USA) and used without further purification.

2.1.1. Preparation of aqueous extract

I. cylindrica was collected from a special area in Universiti Teknologi MARA, Shah Alam, 40450 Selangor, Malaysia. Taxonomy identification on the plant was carried out by Forest Research Institute Malaysia (Sample No. PID 200916-17). The leaves were washed thoroughly to remove dust particles. The leaves were subsequently dried in a laboratory hot air oven at 60°C for 72 min and then ground into a fine powder using Waring laboratory dry mill. The coarse leaf powder was then sifted using a 100-mesh sieve to obtain a soluble powder. Approximately 5 g of powder was weighed and mixed with 200 ml of ultrapure water. The mixture was stirred and heated in a water bath at 60°C for 30 min before filtered using Whatman No. 1 filter paper. The supernatant collected is assumed as 100% concentration and was further diluted as needed. Fig. 1 shows the preparation of green reducing agent from *I. cylindrica* leaves [10].

2.1.2. Biosynthesis of silver nanoparticles

Biosynthesis of silver nanoparticles was conducted out using *I. cylindrica* aqueous extract as a green reducing agent. The synthesis was carried out by adding 10 ml of aqueous *I. cylindrica* extract into 90 ml of 1 mM silver nitrate. The reaction was carried out at 60°C for 10 min and left for 12 h at room temperature before UV-vis characterization. The colloid was labeled as sample SNP01. The appearance of brown color indicates the formation of silver nanoparticles and verification was carried out using UV-visible spectroscopy.

2.1.3. Plant extract concentration

I. cylindrica extract was diluted with ultra-purified water to prepare 10% and 50% extract concentration. The synthesis of silver nanoparticles was carried out by adding 1 mM of silver nitrate to each of the extract concentration (sample SNP02 and SNP03).

2.1.4. Silver salt concentration

The synthesis of silver nanoparticles was repeated using a 10% aqueous *I. cylindrica* extract. The extract was introduced
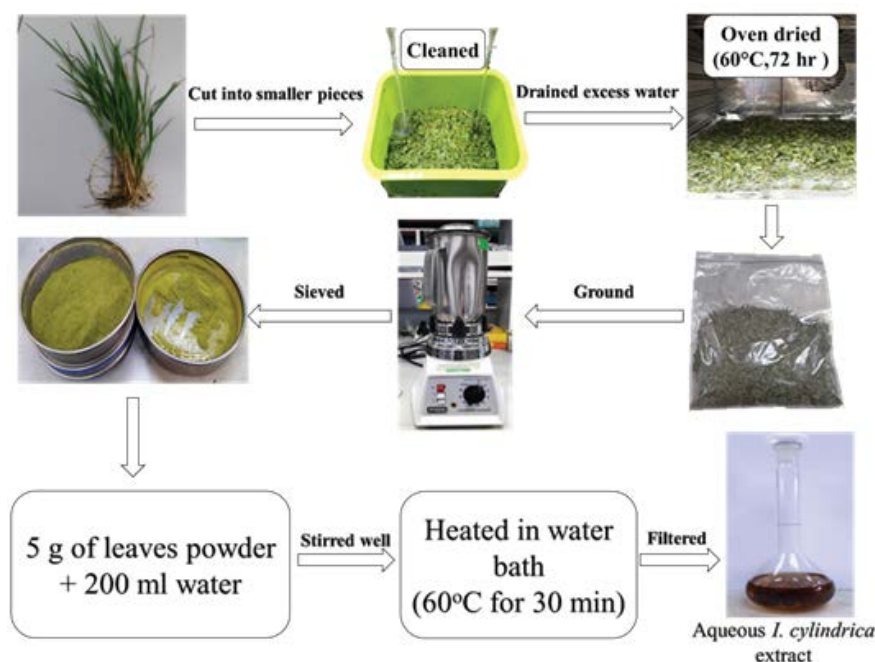

Fig. 1. Preparation of green reducing agent from *Imperata cylindrica* leaves.

to 5 and 10 mM of silver nitrate. The colloids were labeled as sample SNP04 and SNP05.

2.1.5. Reaction temperature

Silver nanoparticles were synthesized by adding 10% aqueous *I. cylindrica* into 10 mM of aqueous silver nitrate in a beaker. The mixtures were incubated in a water bath at 30°C and 100°C. The colloids were labeled as sample SNP06 and SNP07 respectively.

2.1.6. pH of the medium

The pH of the reaction mixture of each set was varied by adding NaOH and HCl dropwise until pH 3, pH 7 and pH 10 were obtained and labeled as sample SNP08, SNP09, and SNP10, respectively.

2.2. Characterization of silver nanoparticles

2.2.1. UV-visible analysis

Qualitative analysis of silver nanoparticles surface plasmon resonance (SPR) was performed using a UV-vis spectrophotometer (Perkin Elmer, Lambda 35 UV/VIS System, Malaysia), equipped with a tungsten-halogen and deuterium lamp as a light source. Each silver nanoparticles mixture was diluted 10 times with ultra-pure water before filled into 1 cm quartz cuvette. The absorbance was scanned between 200–800 nm [18,19].

2.2.2. Dynamic light scattering analysis

Hydrodynamic diameter (d_H) and polydispersity index (PDI) of biosynthesized silver nanoparticles were measured using a Malvern nano-size particle analyzer in the range of between 0.1 nm to 10 μm. The following analysis conditions were adopted; particle refractive 1.590, particle absorption coefficient 0.01, water refractive index 1.33 and viscosity 0.8872 [11]. The measurement was done at a temperature of 25°C by filling approximately 1 mL of biosynthesized silver nanoparticles sample into a disposable cuvette. Thirteen measurement cycles of 10 s each were recorded and then averaged by using a computer program (DTS, Ver. 5.00 from Malvern). Two pieces of information obtained from this study are the mean value for the size (Z-Average) and PDI.

2.2.3. Field scanning electron microscopy analysis

In this study, a micrograph of biosynthesized silver nanoparticles was acquired using a field scanning electron microscope (Jeol JSM-6701, Malaysia). The colloidal silver was purified and centrifuged at 700 rpm for 15 min before it was dried in a hot air oven for 24 h at 80°C [10]. The examination of the sample was performed by mounting powdered nanoparticles on a specimen stub with a double-sided carbon adhesive tape and coated with gold in a sputter coater [12]. The micrograph of silver nanoparticles was captured at 50 and 100 K magnification with an accelerating voltage of 15 kV. The instrument utilized the Everhart-Thornley detector to form an image and create topographic contrast [13]. Elemental characterization of successfully synthesized silver nanoparticles was carried out using energy dispersive X-ray

(EDX) spectroscopy. The sample that has been previously prepared for field scanning electron microscopy (FESEM) analysis was analyzed using the EDX unit attached to the FESEM instrument.

2.2.4. X-ray diffraction analysis

X-ray diffraction (XRD) pattern of dry nanoparticle powder was obtained using PANalytical X-Pert Pro XRD machine with CuKα radiation of wavelength 1.541° and scanning angle 2θ over the range of 10°–80°.

3. Result and discussion

3.1. Biosynthesis of silver nanoparticles using I. cylindrica extract

Generally, biosynthesis of silver nanoparticles using aqueous *I. cylindrica* extract gave a characteristic color change from yellow to dark brown with an absorption maximum in the range of 441–446 nm attributed to the SPR band of silver nanoparticles [20,21]. Previous studies show that the absorption intensified with increasing formation of silver nanoparticles [22]. The position of maximum absorption wavelength is correlated to the size of the synthesized silver nanoparticles [23–25]. Typically, an increase in particle size and formation of large silver aggregates will shift the position of maximum absorption to longer wavelength (redshift) [26]. On the other hand, a decrease in particle size resulted in the shifting of maximum absorption to shorter wavelength (blue shift) [27]. Based on the SPR spectrum of sample SN01-SN05, there should be no significant difference in the shape of the nanoparticles synthesized. This assumption is motivated by Mie's theory that stated small spherical nanocrystal (Ag or Au) exhibit only a single SPR band [28,29].

Analysis of the silver nanoparticles colloids via dynamic light scattering (DLS) gave the average particle diameter size and PDI which is a dimensionless value and scaled from 0.05 to 0.70, whereby value approaching 0.05 is considered as monodisperse while a value greater than 0.70 indicates that the sample has a very broad distribution [30]. From DLS measurement, silver nanoparticles synthesized using *I. cylindrica* extract have a diameter in the range of 174.30–28.55 nm with PDI less than 0.58.

The morphology and elemental compositions of silver nanoparticles were then confirmed using FESEM-EDX. The crystalline nature of silver nanoparticles was confirmed by XRD studies (Fig. 2a). The XRD pattern (Fig. 2b) recorded from the biosynthesized silver nanoparticles showed a very intense Bragg reflection at 38.18, 44.41, 64.55 and 77.56 degrees corresponding to (111), (200), (220) and (311) crystal lattice of face-centered cubic silver [31].

Generally based on the characterization data, the biosynthesized silver nanoparticles have a similar attribute to silver nanoparticles synthesized via conventional reducing agents [32].

In our previous work using *Hibiscus rosa sinensis* leaves extract, the particles were irregular in shape. On the other hand, the use of *I. cylindrica* extract allows the formation of nearly spherical and uniform particles which are desirable for certain application. The biosynthesized silver nanoparticles
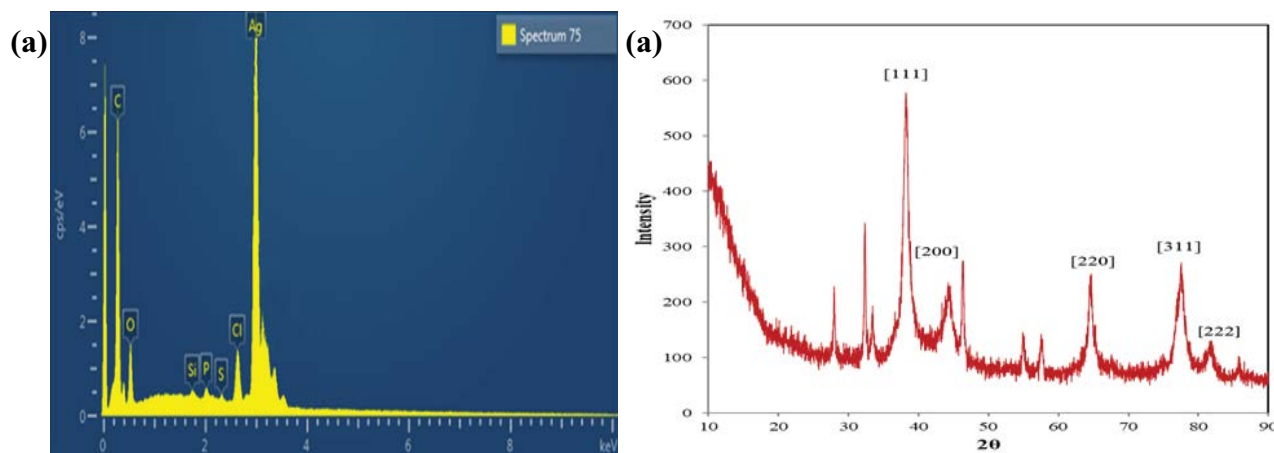
Fig. 2. (a) EDX spectrum and (b) XRD diffractogram of silver nanoparticles synthesized by aqueous extract of *Imperata cylindrica*.

have the potential to be incorporated in health industries as *I. cylindrica* extract is nontoxic and possess medicinal properties [14].

3.2. Optimization of biosynthesized silver nanoparticles

Manipulation of synthesis parameters which include plant extract concentration, silver salt concentration, reaction temperature and pH of the medium, produced samples with various sizes, morphology, and dispersity. The effect of each parameter was studied and optimum parameters for obtaining a monodisperse population of silver nanoparticles were proposed.

3.3. Plant extract concentration

Silver nanoparticles were synthesized using 10%, 50%, and 100% (sample code SNP01, SNP02, and SNP03) (Fig. 3b) concentration of aqueous extract of *I. cylindrica*. As the concentration of extract increased, the SPR band (Fig. 3a) intensified and absorption maximum shifted to lower wavelengths (446, 443 and 428 nm). These findings indicate the increase in the formation of nanoparticles [24] and the decrease of particle size due to the presence of more biomolecules at higher plant extract concentration [25–27]. Analysis of particle size using DLS also showed a similar trend in which the particles formed at 50% (SNP02) and 100% (SNP03) plant extract concentration measured 33.79 and 28.55 nm respectively.

The FESEM micrographs (Figs. 3c–e) justified that the particles are spherical with more apparent agglomeration as the concentration of plant extract increases. The agglomeration is probably the reason for the increase in PDI value as (SNP02 = 0.30 and SNP03 = 0.58) the concentration of extract increases. Earlier studies have revealed a strong correlation between the size of metal nanoparticles and capping agent to metal ion concentration ratio [28]. An increase in plant concentration provides an excess amount of reducing agent which causes insufficient Ag$^+$ for a reaction. As a consequence, nucleation and growth would compete with each other for the metal ion. Therefore, it was proposed that the decrease of size at a high temperature is a result of the

increase in nucleation leading to an insufficient precursor for particle growth. It was also observed that samples SNP02 and SNP03 aggregated into larger particles easier, due to their small particle size. Generally, the aggregation barrier increases with increasing size, therefore, providing more resistance towards aggregation [6]. Based on the acceptable size and lowest indication of polydispersity in sample SNP01, 10% was considered as an optimal concentration aqueous plant extract.

3.4. Silver salt concentration

Silver nitrate of 5 and 10 mM were used to synthesize samples SNP04 and SNP05 using 10% plant extract (Fig. 4b). The absorption intensity increases when 5 mM of AgNO$_3$ was used, which indicates the formation of more silver nanoparticles [14]. The absorption maximum of the SPR band (Fig. 4a) of SNP04 and SNP04 was shifted to a lower wavelength (441 nm). Although both samples were blue-shifted, only SN04 showed a size reduction (38.93 nm). However, despite having a slightly larger diameter (54.41 nm), SN05 is highly monodisperse (PDI = 0.12) compared to SN04 (PDI = 0.34). At an increasing concentration of silver nitrate, the nucleation rate reached an optimal level [14]. Although the further increase in silver salt concentration causes the particle to have a relatively bigger size, the stability towards aggregation also increases [6]. This is also supported by the FESEM micrograph (Figs. 4c and d) which showed particles that are well distributed with uniform size and shape.

3.5. Reaction temperature

Synthesis of silver nanoparticles was carried out using a 10% concentration of plant extract with 10 mM of AgNO$_3$ at 30°C and 100°C (sample code SNP06 and SNP07) (Fig. 5b). At a relatively low temperature, the synthesis of silver nanoparticles took a longer time. Sample SNP06 (60°C) exhibited color transformation after approximately 6 h, whereas sample SNP07 (100°C) transformed after 5 min. This is because, at increasing temperature, reactants were rapidly consumed [29], allowing a quicker change in the color of the
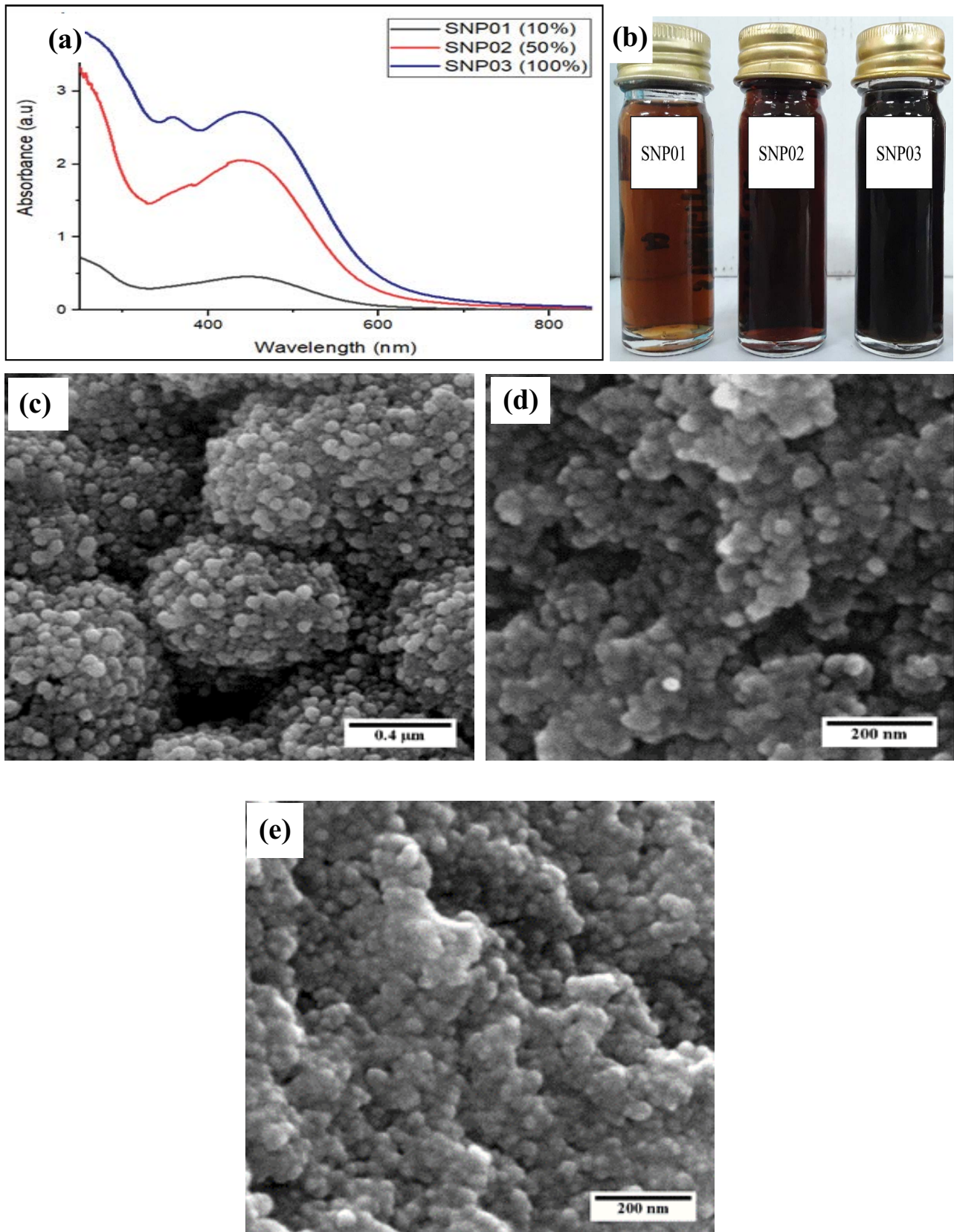
Fig. 3. (a) UV-Visible absorption spectra, (b) samples SNP01, SNP02, and SNP03 while (c,d,e) FESEM micrograph for samples SNP01, SNP02 and SNP03 respectively.
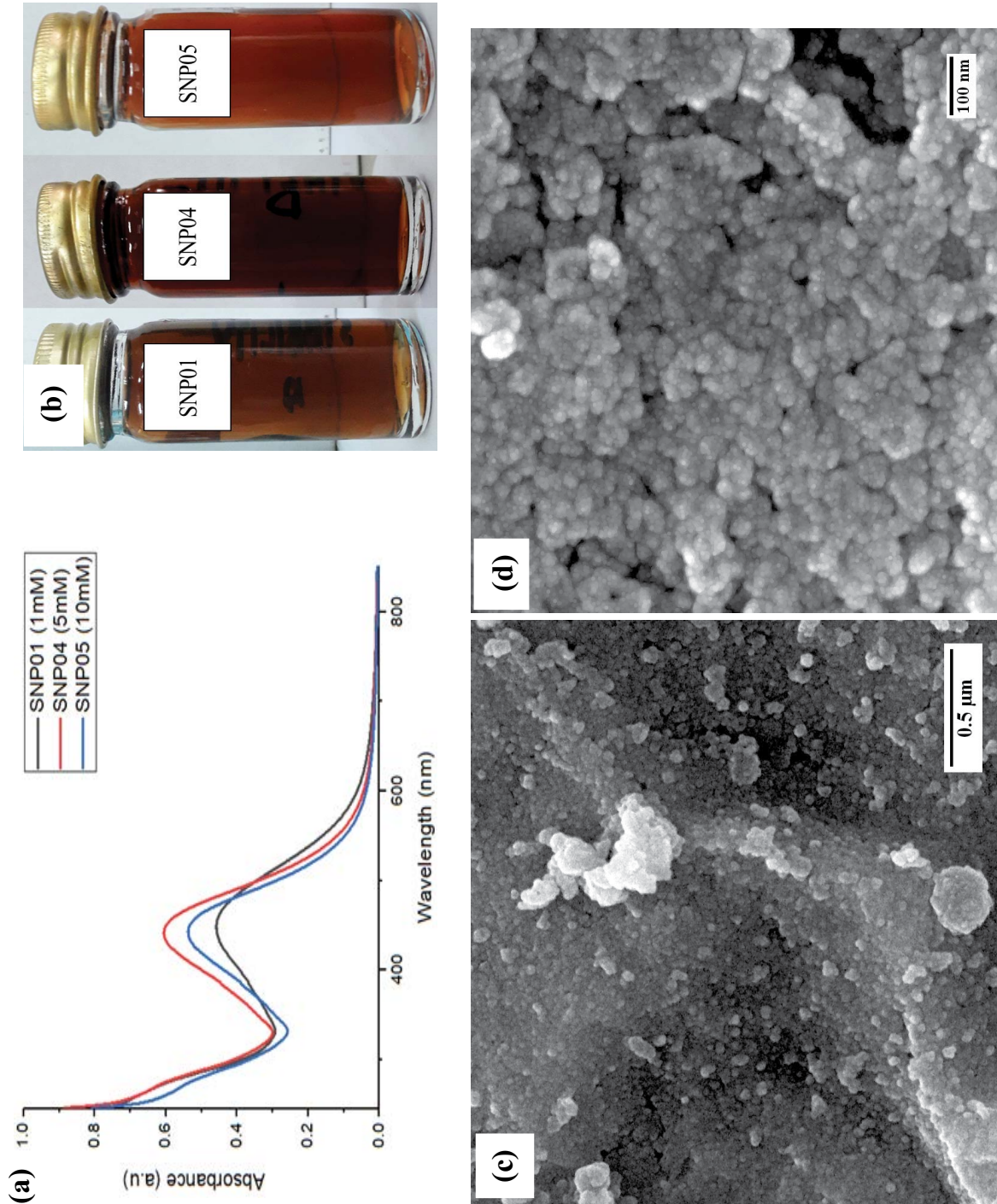
Fig. 4. (a) UV-Visible absorption spectra, (b) samples SNP01, SNP04, and SNP05 while (c) and (d) and FESEM micrograph for samples SNP04 and SNP05 respectively.

Table 1
Effect of various parameters on average size and polydispersity of biosynthesized silver

Sample code	Synthesis parameter				Result	
	Plant extract concentration (%)	Silver salt concentration (mM)	pH	Temperature (°C)	Average diameter	PDI
Effect of plant extract concentration (%)						
SNP01	10	1	5.3	60	41.87	0.19
SNP02	50	1	5.3	60	33.79	0.30
SNP03	100	1	5.3	60	28.55	0.58
Effects of silver salt concentration (mM)						
SNP01	10	1	5.3	60	41.87	0.19
SNP04	10	5	5.3	60	38.93	0.34
SNP05	10	10	5.3	60	54.41	0.12
Effect of reaction temperature (°C)						
SNP05	10	10	5.3	60	54.41	0.12
SNP06	10	10	5.3	30	41.28	0.29
SNP07	10	10	5.3	100	61.91	0.35
pH of medium						
SNP05	10	10	5.3	60	54.41	0.12
SNP08	10	10	3	60	174.30	0.19
SNP09	10	10	7	60	120.30	0.20
SNP10	10	10	10	60	117.60	0.22

solution [24]. The samples have a similar absorption pattern as shown in Fig. 5a after optimization of the concentration of both silver salt and plant extract concentration was carried out. The maximum absorbance of SNP06 (30°C) was shifted to a lower wavelength (443 nm) while SNP07 absorbed at a slightly longer wavelength (445 nm). The DLS analysis revealed that SNP06 has a smaller particle size (41.28 nm) than SNP07 (61.91 nm).

Previously published literature suggested the reduction of particle size with the increase in reaction temperature. Contrary to the earlier finding, it was discovered in this study that by increasing the reaction temperature (100°C), an increase in particle size was obtained. This is probably due to the presence of abundant Ag^+ ions which encourage the excessive formation of the crystal nucleus, thus allowing the nanoparticles to grow bigger when the heat is continuously supplied [30]. However, at low reaction temperature (30°C), nucleation and growth of particles occur slowly due to the absence of heat. In addition, collision frequency among metal precursors [14] that causes particles to aggregate into larger particles is reduced. However, the drawback of synthesizing silver nanoparticles at a lower temperature (30°C) is the long reaction time which might cause an increase in polydispersity (PDI = 0.35). Furthermore, it was observed that SNP05 which was synthesized at 60°C have smaller PDI (0.12) when compare to SNP07 (100°C). This suggested that the most optimal temperature for synthesizing silver nanoparticles is 60°C. This temperature allows the formation of highly monodisperse nanoparticles at a reasonable reaction time (30 min).

3.6. pH of the medium

Biosynthesis of silver nanoparticles by *I. cylindrica* extract is most feasible at its original pH 5.7. With regard to this study, synthesizing silver nanoparticles at pH 3, 7 and 10 (samples SN08, SN09, and SN10) does not result in a clear absorption peak in UV-visible analysis (Fig. 6a). Sample SN08 which was synthesized at pH 3 changed to the faint grey solution (Fig. 6b), exhibiting a weak absorption (Fig. 6a) indicating that the formation of silver nanoparticles was not feasible [24]. Contrary, at pH 7 and 10, the reaction occurred instantaneously, forming a deep brown solution (Fig. 6b).

Analysis of samples SN08, SN09 and SN10 via DLS revealed the formation of large particles with an average diameter of 174.30, 120.30 and 117.60 nm. The PDI of the samples are almost similar (0.19–0.22). Nevertheless, modification of reaction pH in this study resulted in excessive particle enlargement which is not desirable since nanoparticles are defined as particles measuring less than 100 nm. Micrographs from FESEM (Figs. 6c and d) showed the formation of large particles and agglomerates within samples. As reported in the previous study [24,31] changing pH of the medium affected the shape and size of the particles since it has the ability to alter the charge of a biomolecule which might affect their capping and stabilizing abilities. In addition, there is a possibility that stabilization of silver nanoparticles synthesized via plant extract is provided by natural polymers such as tannins, could not withstand acidic medium [32] which eventually leads to loss of stabilization towards nanoparticles, hence causing agglomeration.
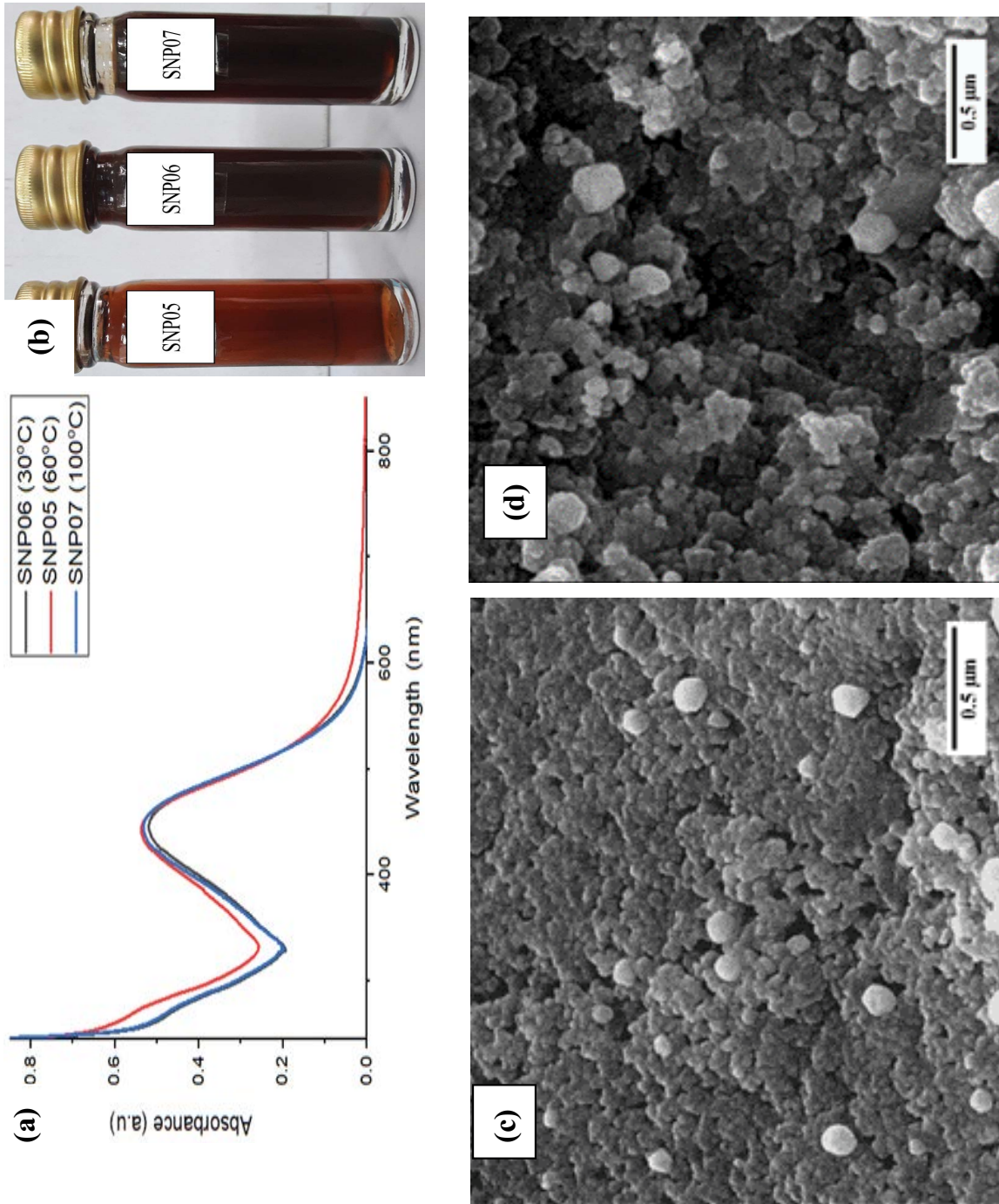
Fig. 5. (a) UV-Visible absorption spectra (b) samples SNP05, SNP06, and SNP07 while (c) and (d) and FESEM micrograph for samples SNP06 and SNP07 respectively.
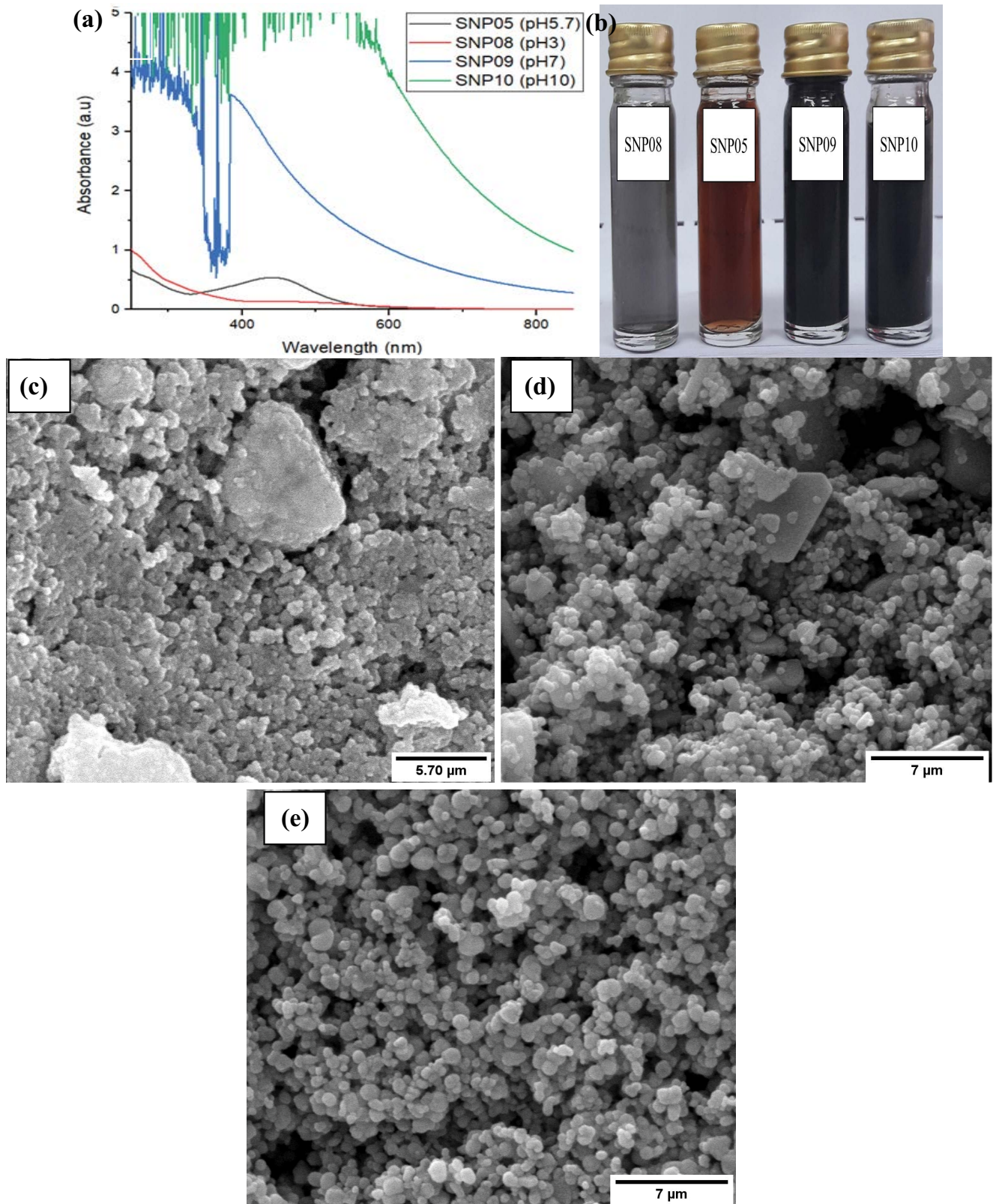
Fig. 6. (a) UV-Visible absorption spectra, (b) samples SNP08, SNP05, SNP09, and SNP10 while (c,d,e) are FESEM micrograph for samples SNP08, SNP09 and SNP10 respectively. (**spectrum too noisy).

This can be observed from the noise shown in UV-Vis measurement due to interference from large particles. All results are summarized in Table 1.

4. Conclusion

This study demonstrated that the biosynthesis of silver nanoparticles using an aqueous extract of *I. cylindrica* is possible and simpler than other green techniques or conventional methods. Optimization of synthesis parameters namely plant extract concentration, silver salt concentration, reaction temperature, and pH can lead to the formation of a monodisperse population of a single geometry silver nanoparticle. The most favorable condition for synthesizing silver nanoparticles from aqueous leaves extract of *I. cylindrica* is by using only 10% of the extract with 10 mM of silver nitrate. The reaction should be carried out at 60°C with no pH adjustment.

References

[1] K.L. Kelly, E. Coronado, L.L. Zhao, G.C. Schatz, The optical properties of metal nanoparticles: the influence of size, shape, and dielectric environment, J. Phys. Chem., 107 (2003) 668–677.

[2] A.B. Afzal, M.J. Akhtar, M. Nadeem, M.M. Hassan, Investigation of structural and electrical properties of polyaniline/gold nanocomposites, J. Phys. Chem. C, 113 (2009) 17560–17565.

[3] Y. Xia, H. Yang, C.T. Campbell, Nanoparticles for catalysis, Acc. Chem. Res., 46 (2013) 1671–1672.

[4] G. Merga, R. Wilson, G. Lynn, B.H. Milosavljevic, D. Meisel, Redox catalysis on "naked" silver nanoparticles, J. Phys. Chem. C, 111 (2007) 12220–12226.

[5] B. Calderón-Jiménez, G.F. Sarmanho, K.E. Murphy, A.R.M. Bustos, J.R. Vega-Baudrit, NanoUV-VIS: an interactive visualization tool for monitoring the evolution of optical properties of nanoparticles throughout synthesis reactions, J. Res. Nat. Inst. Stand. Technol., 122 (2017) 1–10.

[6] J. Polte, Fundamental growth principles of colloidal metal nanoparticles – a new perspective, CrystEngComm, 17 (2015) 6809–6830.

[7] G.E. MacDonald, Cogongrass (*Imperata cylindrica*)—biology, ecology, and management, Crit. Rev. Plant Sci., 23 (2004) 367–380.

[8] A.M. Fayaz, K. Balaji, P.T. Kalaichelvan, R. Venkatesan, Fungal based synthesis of silver nanoparticles—an effect of temperature on the size of particles, Colloids Surf., B, 74 (2009) 123–126.

[9] M.B. Kasture, P. Patel, A.A. Prabhune, C.V. Ramana, A.A. Kulkarni, B.L.V. Prasad, Synthesis of silver nanoparticles by sophorolipids: effect of temperature and sophorolipid structure on the size of particles, J. Chem. Sci., 120 (2008) 515–520.

[10] M. Vanaja, K. Paulkumar, M. Baburaja, S. Rajeshkumar, G. Gnanajobitha, C. Malarkodi, M. Sivakavinesan, G. Annadurai, Degradation of methylene blue using biologically synthesized silver nanoparticles, Bioinorg. Chem. Appl., 2014 (2014) 8 pages.

[11] S. Saha, J. Sarkar, D. Chattopadhyay, S. Patra, A. Chakraborty, K. Acharya, Production of silver nanoparticles by a phytopathogenic fungus *bipolaris nodulosa* and its antimicrobial activity, Dig. J. Nanomater. Biostructures, 5 (2010) 887–895.

[12] S. Hamedi, S.M. Ghaseminezhad, S.A. Shojaosadati, S. Shokrollahzadeh, Comparative study on silver nanoparticles properties produced by green methods, Iran. J. Biotechnol., 10 (2012) 191–197.

[13] M. de A. Pereira-da-Silva, F.A. Ferri, Scanning Electron Microscopy, in: Nanocharacterization Techniques, 1st ed., A.L. Da Róz, M. Ferreira, F. de L. Leite, O.N.O. Jr., Eds., Matthew Deans, 2017, p. 8. Available at: https://www.elsevier.com/books/nanocharacterization-techniques/de-oliveira-jr/978-0-323-49778-7.

[14] A. Sobczak-Kupiec, D. Malina, Z. Wzorek, M. Zimowska, Influence of silver nitrate concentration on the properties of silver nanoparticles, IET Micro Nano Lett., 6 (2011) 656.

[15] S. Agnihotri, S. Mukherji, S. Mukherji, Size-controlled silver nanoparticles synthesized over the range 5–100 nm using the same protocol and their antibacterial efficacy, R. Soc. Chem., 4 (2014) 3974–3983.

[16] A. Slistan-Grijalva, R. Herrera-Urbina, J.F. Rivas-Silva, M. Ávalos-Borja, F.F. Castillón-Barraza, A. Posada-Amarillas, Assessment of growth of silver nanoparticles synthesized from an ethylene glycol–silver nitrate–polyvinylpyrrolidone solution, Physica, 25 (2005) 438–448.

[17] S.L. Smitha, K.M. Nissamudeen, D. Philip, K.G. Gopchandran, Studies on surface plasmon resonance and photoluminescence of silver nanoparticles, Spectrochim. Acta, Part A, 71 (2008) 186–190.

[18] E.D.R. Angelina, R. Bavyaa, R. Rajagopal, Green synthesis and characterization of silver nanoparticles using fenugreek seed extract, Int. J. Sci. Res. Publ., 3 (2013) 7–9.

[19] U.P. Azad, V. Ganesan, M. Pal, Catalytic reduction of organic dyes at gold nanoparticles impregnated silica materials: influence of functional groups and surfactants, J. Nanopart. Res., 13 (2011) 3951–3959.

[20] B. Ajitha, Y. Ashok Kumar Reddy, P. Sreedhara Reddy, Biosynthesis of silver nanoparticles using *Momordica charantia* leaf broth: evaluation of their innate antimicrobial and catalytic activities, J. Photochem. Photobiol., B, 146 (2015) 1–9.

[21] G. Mie, Contributions to the optics of turbid media, particularly of colloidal metal solutions, Ann. D. Phys., 25 (1998) 377–413.

[22] Malvern, Inform white paper dynamic light scattering, Malvern Guid., 5 (2011) 6.

[23] M. Amin, F. Iram, M.S. Iqbal, M.Z. Saeed, M. Raza, S. Alam, Arabinoxylan-mediated synthesis of gold and silver nanoparticles having exceptional high stability, Carbohydr. Polym., 92 (2013) 1896–1900.

[24] A. Verma, M.S. Mehata, Controllable synthesis of silver nanoparticles using Neem leaves and their antimicrobial activity, J. Radiat. Res. Appl. Sci., 9 (2016) 109–115.

[25] A.A. Moosa, A.M. Ridha, M. Al-Kaser, Process parameters for green synthesis of silver nanoparticles using leaves extract of aloe vera plant, Int. J. Multidiscip. Curr. Res., 3 (2015) 966–975.

[26] M. Sathishkumar, K. Sneha, S.W. Won, C.-W. Cho, S. Kim, Y.-S. Yun, *Cinnamon zeylanicum* bark extract and powder mediated green synthesis of nano-crystalline silver particles and its bactericidal activity, Colloids Surf., B, 73 (2009) 332–338.

[27] L. Christensen, S. Vivekanandhan, M. Misra, A.K. Mohanty, Biosynthesis of silver nanoparticles using *Murraya koenigii* (curry leaf): an investigation on the effect of broth concentration in reduction mechanism and particle size, Adv. Mater. Lett., 2 (2011) 429–434.

[28] S.K. Das, A.R. Das, A.K. Guha, Microbial synthesis of multishaped gold nanostructures, Small, 6 (2010) 1012–1021.

[29] S.-W. Kim, J.N. Park, Y.J. Jang, Y.H. Chung, S.J. Hwang, T.W. Hyeon, Y.W. Kim, Synthesis of monodisperse palladium nanoparticles, Nano Lett., 3 (2003) 1289–1291.

[30] H.Y. Liu, H. Zhang, J. Wang, J.F. Wei, Effect of temperature on the size of biosynthesized silver nanoparticle: deep insight into microscopic kinetics analysis, Arabian J. Chem., 10 (2017), https://doi.org/10.1016/j.arabjc.2017.09.004 (In Press).

[31] M.M.H. Khalil, E.H. Ismail, F. El-Magdoub, Biosynthesis of Au nanoparticles using olive leaf extract: 1st nano updates, Arabian J. Chem., 5 (2012) 431–437.

[32] O. Velgosová, A. Mražíková, R. Marcinčáková, Influence of pH on green synthesis of Ag nanoparticles, Mater. Lett., 180 (2016) 336–339.